3-D Simulations of Ergospheric Disk Driven Poynting Jets

Brian Punsly

4014 Emerald Street No.116, Torrance CA, USA 90503 and International Center for Relativistic Astrophysics, I.C.R.A.,University of Rome La Sapienza, I-00185 Roma, Italy

brian.m.punsly@L-3com.com or brian.punsly@gte.net

ABSTRACT

This Letter reports on 3-dimensional simulations of Kerr black hole magnetospheres that obey the general relativistic equations of perfect magnetohydrodynamics (MHD). In particular, we study powerful Poynting flux dominated jets that are driven from dense gas in the equatorial plane in the ergosphere. The physics of which has been previously studied in the simplified limit of an ergopsheric disk. For high spin black holes, $a/M > 0.95$, the ergospheric disk is prominent in the 3-D simulations and is responsible for greatly enhanced Poynting flux emission. Any large scale poloidal magnetic flux that is trapped in the equatorial region leads to an enormous release of electromagnetic energy that dwarfs the jet energy produced by magnetic flux threading the event horizon. The implication is that magnetic flux threading the equatorial plane of the ergosphere is a likely prerequisite for the central engine of powerful FRII quasars.

Subject headings: Black hole physics - magnetohydrodynamics -galaxies: jets— galaxies: active — accretion disks

1. Introduction

Recent studies of luminous radio quasars indicate that the power of the radio jet can exceed the bolometric luminosity associated with the accretion flow thermal emission (Punsly 2006b, 2007). This has proven to be quite challenging for current 3-D numerical simulations of MHD black hole magnetospheres. Based on table 4 of Hawley and Krolik (2006) and the related discussion of Punsly (2006b, 2007), the most promising 3-D simulations for achieving this level of efficiency are those of the highest spin, $a/M \approx 1$ (where the black hole mass, M, and the angular momentum per unit mass, a, are in geometrized units). More generally, such high spins have been inferred in some black hole systems based on observational constraints (McClintock et al 2006). Thus, there is tremendous astronomical relevance to these highest

spin configurations, in particular the physical origin of the relativistic Poynting jet. The first generation of long term 3-D simulations produced one Poynting flux powerhouse, the $a/M = 0.995$ simulation, KDE (De Villiers et al 2003, 2005a; Hirose et al 2004; Krolik et al 2005). The source of most of the Poynting flux was clearly shown to be outside the event horizon in KDE (Punsly 2006a). However, without access to the original data, the details of the physical mechanism could not be ascertained. A second generation of 3-D simulations were developed in Hawley and Krolik (2006), the highest spin case was KDJ, $a/M = 0.99$, with by far the most powerful Poynting jet within the new family of simulations; three times the Poynting flux (in units of the accretion rate of mass energy) of the next closest simulation KDH, $a/M = 0.95$. The last three data dumps, at simulation times, t = 9840 M, t = 9920 M and t = 10000 M, were generously made available to this author. The late time behavior of the simulations is established after t = 2000 M (when the large transients due to the funnel formation have died off) making these data dumps of particular interest for studying the Poynting jet (Hawley and Krolik 2006). This paper studies the origin of the Poynting jet at these late times.

The analysis of the data from the KDJ simulation clearly indicates that the Poynting flux in the outgoing jet is dominated by large flares. Typically, one expects the turbulence in the field variables to mask the dynamics of Poynting flux creation in an individual time slice of one of the 3-D simulations (Punsly 2006a). Surprisingly, the flares are of such a large magnitude that they clearly standout above the background field fluctuations as evidenced by figure 1. The flares are created in the equatorial accretion flow deep in the egosphere between the inner calculational boundary at r=1.203 M and r= 1.6 M (the event horizon is at r= 1.141 M). Powerful beams of Poynting flux emerge perpendicular to the equatorial plane in the ergospheric flares and much of the energy flux is diverted outward along approximately radial trajectories that are closely aligned with the poloidal magnetic field direction in the jet (see figure 1). The situation is unsteady, whenever some vertical magnetic flux is captured in the accretion flow it tends to be asymetrically distributed and concentrated in either the northern or southern hemisphere. This hemisphere then receives a huge injection of electromagnetic energy on time scales $\sim 60M$.

The source of Poynting flux in KDJ resembles a nonstationary version of the ergospheric disk (see Punsly and Coroniti (1990) and chapter 8 of Punsly (2001) for a review). The ergospheric disk is modeled in the limit of negligible accretion and it is the most direct manifestation of gravitohydromagnetics (GHM) Punsly (2001). A GHM dynamo arises when the magnetic field impedes the inflow of gas in the ergosphere, i.e., vertical flux in an equatorial accretion flow. The strong gravitational force will impart stress to the magnetic field in an effort to move the plasma through the obstructing flux. In particular, the metric induced frame dragging force will twist up the field azimuthally. These stresses are coupled

into the accretion vortex around a black hole by large scale magnetic flux, and propagate outward as a relativistic Poynting jet. The more obstinate the obstruction, the more powerful the jet. There are two defining characteristics that distinguish the GHM dynamo from a Blandford-Znajek (B-Z) process, Blandford and Znajek (1977), on field lines that thread the ergopshere:

1. The B-Z process is electrodynamic so there is no source within the ergosphere, it appears as if the energy flux is emerging from the horizon. In the GHM mechanism, the source of Poynting flux is in the ergospheric equatorial accretion flow.

2. In a B-Z process in a magnetosphere shaped by the accretion vortex, the field line angular velocity is, $\Omega_F \approx \Omega_H/2$ (where Ω_H is the angular velocity of the horizon) near the pole and decreases with latitude to $\approx \Omega_H/5$ near the equatorial plane of the inner ergosphere (Phinney 1983). In GHM, since the magnetic flux is anchored by the inertia of the accretion flow in the inner ergosphere, frame dragging enforces $d\phi/dt \approx \Omega_H$. One therefore has the condition, $\Omega_F \approx \Omega_H$.

In order to understand the physical origin of the Poynting flux, these two issues are studied below.

2. The KDJ Simulation

The simulation is performed in the Kerr metric (that of a rotating, uncharged black hole), $g_{\mu\nu}$. Calculations are carried out in Boyer-Lindquist (B-L) coordinates (r, θ, ϕ, t). The reader should refer to Hawley and Krolik (2006) for details of the simulation. We only give a brief overview. The initial state is a torus of gas in equilibrium that is threaded by concentric loops of weak magnetic flux that foliate the surfaces of constant pressure. The magnetic loops are twisted azimuthally by the differentially rotating gas. This creates significant magnetic stress that removes angular momentum from the gas, initiating a strong inflow that is permeated by magneto-rotational instabilities (MRI). The end result is that after t = a few hundred M, accreted poloidal magnetic flux gets trapped in the accretion vortex or funnel (with an opening angle of $\sim 60^\circ$ at the horizon tapering to $\sim 35^\circ$ at $r > 20M$). This region is the black hole magnetosphere and it supports a Poynting jet. The surrounding accretion flow is very turbulent.

In order to understand the source of the strong flares of radial Poynting flux, one needs to merely consider the conservation of global, redshifted, or equivalently the B-L coordinate evaluated energy flux (Thorne et al 1986). In general, the divergence of the

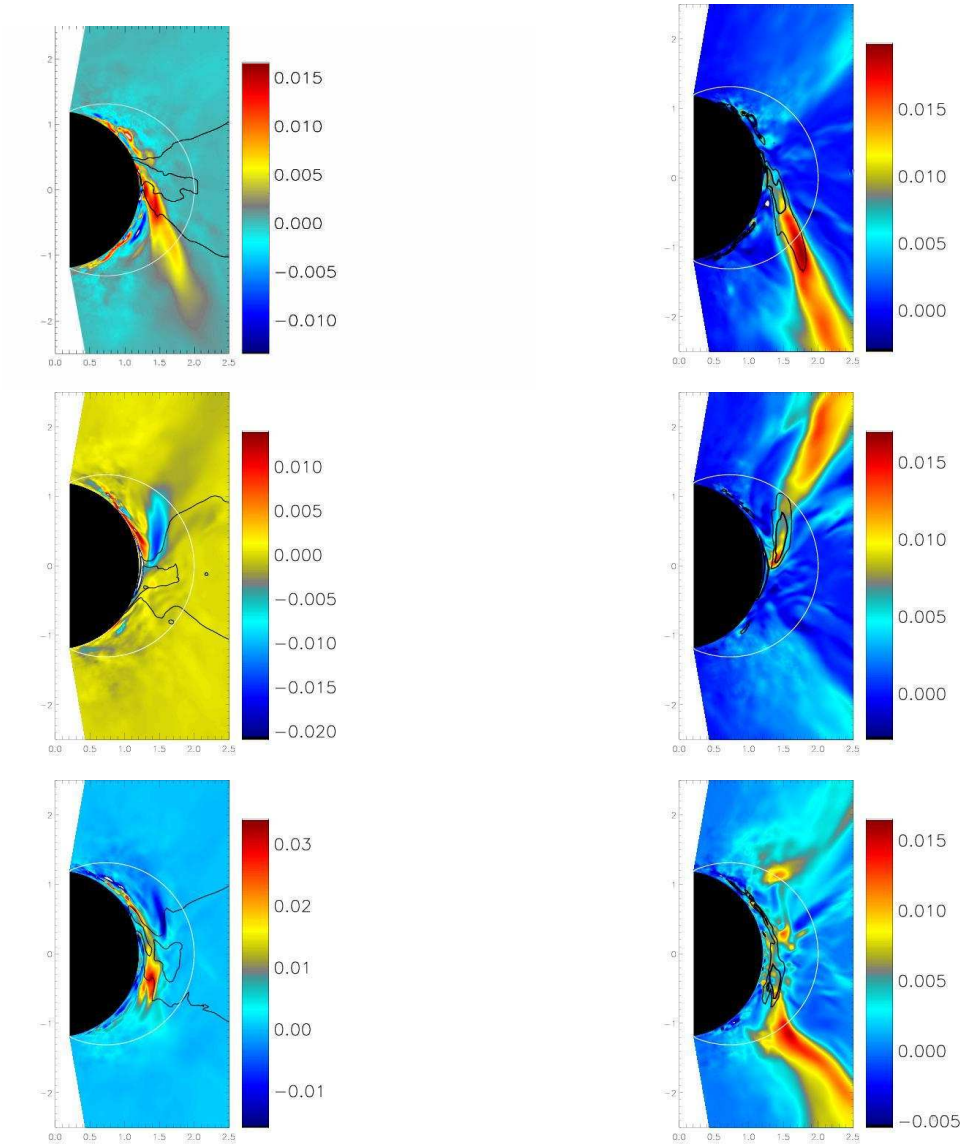

Fig. 1.— The source of Poynting flux. The left hand column is S^θ and the right hand column is S^r in KDJ, both averaged over azimuth, at (from top to bottom) t= 9840 M, t = 9920 M and t= 10000 M. The relative units (based on code variables) are in a color bar to right of each plot for comparison of magnitudes between the six plots. The contours on the S^θ plots are of the density, scaled from the peak value within the frame at relative levels 0.5 and 0.1. The contours on the S^r plots are of S^θ scaled from the peak within the frame at relative levels 0.67 and 0.33. The inside of the inner calculational boundary (r=1.203 M) is black. The calculational boundary near the poles is at 8.1° and 171.9°. Notice that any contribution from an electrodynamic effect associated with the horizon appears minimal. The white contour is the stationary limit surface. There is no data clipping, so plot values that exceed the limits of the color bar appear white.

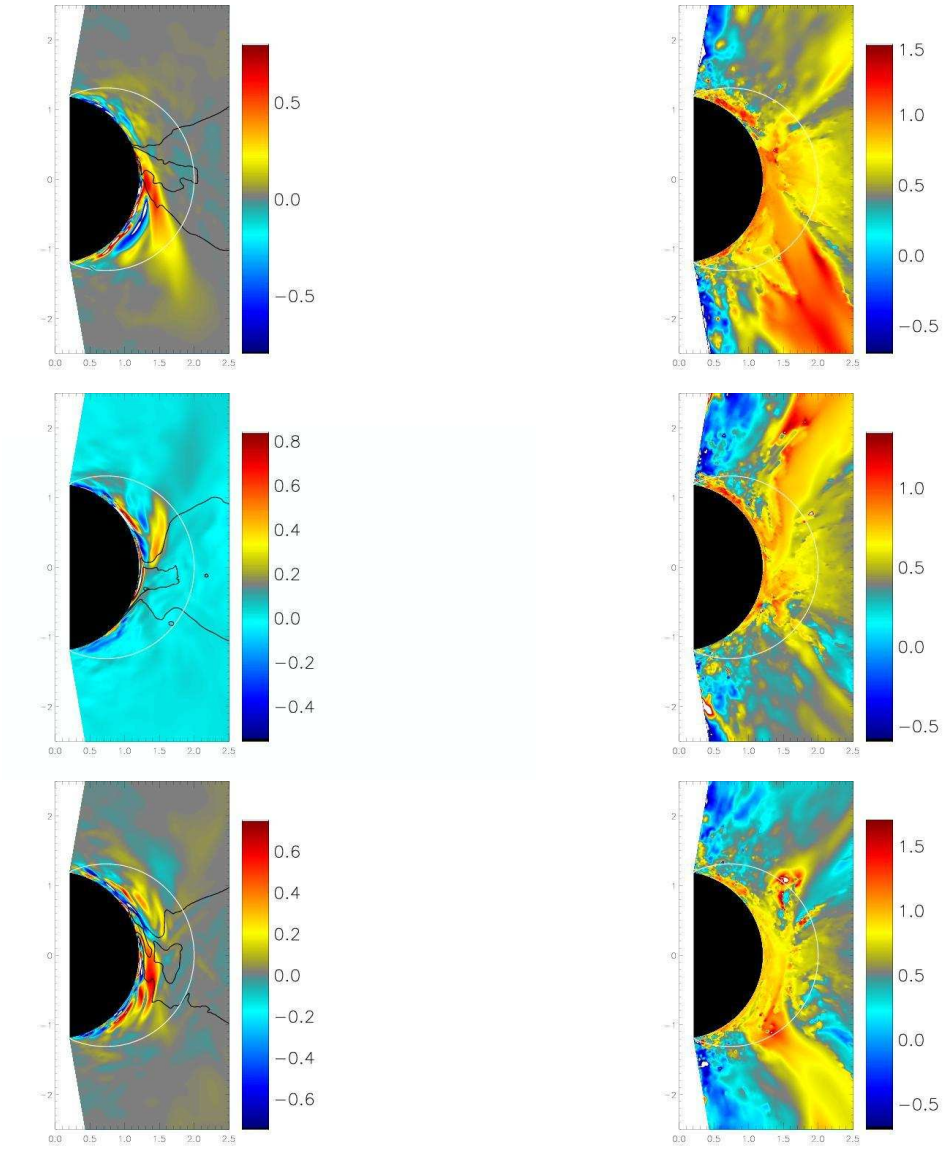

Fig. 2.— The central engine. The left hand column is B^θ and the right hand column is Ω_F in KDJ, both averaged over azimuth, at (from top to bottom) t= 9840 M, t = 9920 M and t= 10000 M. The relative units (based on code variables) are in a color bar to right of each plot for comparison of magnitudes between the plots. The calculational boundaries are the same as figure 1. The contours on the B^θ plots are of the density, scaled from the peak value within the frame at relative levels 0.5 and 0.1. There is no data clipping, so plot values that exceed the limits of the color bar appear white.

time component of the stress-energy tensor in a coordinate system can be expanded as, $T_{t\ ;\nu}^{\ \nu} = (1/\sqrt{-g})[\partial(\sqrt{-g}\,T_t^{\ \nu})/\partial(x^\nu)] + \Gamma^\mu_{\ t\,\beta} T^\beta_\mu$, where $\Gamma^\mu_{\ t\,\beta}$ is the connection coefficient and $g = -(r^2 + a^2\cos^2\theta)^2 \sin^2\theta$ is the determinant of the metric. However, the Kerr metric has a Killing vector (the metric is time stationary) dual to the B-L time coordinate. Thus, there is a conservation law associated with the time component of the divergence of the stress-energy tensor. Consequently, if one expands out the inhomogeneous connection coefficient term in the expression above, it will equate to zero. The conservation of energy evaluated in B-L coordinates reduces to, $\partial(\sqrt{-g}\,T_t^{\ \nu})/\partial(x^\nu) = 0$, where the four-momentum $-T_t^{\ \nu}$ has two components: one from the fluid, $-(T_t^{\ \nu})_{\rm fluid}$, and one from the electromagnetic field, $-(T_t^{\ \nu})_{\rm EM}$. The reduction to a homogeneous equation with only partial derivatives is the reason why the global conservation of energy can be expressed in integral form in (3.70) of Thorne et al (1986). It follows that the poloidal components of the redshifted Poynting flux are $S^\theta = -\sqrt{-g}\,(T_t^{\ \theta})_{\rm EM}$ and $S^r = -\sqrt{-g}\,(T_t^{\ r})_{\rm EM}$. We can use these simple expressions to understand the primary source of the Poynting jet in KDJ. Figure 1 is a plot of S^θ (on the left) and S^r (on the right) in KDJ at the last three time steps of data collection. Each frame is the average over azimuth of each time step. This greatly reduces the fluctuations as the accretion vortex is a cauldron of strong MHD waves. The individual $\phi =$ constant slices show the same dominant behavior, however it is embedded in large MHD fluctuations. On the left hand column of figure 1, density contours have been superimposed on the images to indicate the location of the equatorial accretion flow. The density is evaluated in B-L coordinates with contours at 0.5 and 0.1 of the peak value within $r < 2.5M$. Notice that in all three left hand frames, S^θ is created primarily in regions of very high accretion flow density. In all three of the right hand frames of figure 1, there is an enhanced S^r that emanates from the ergosphere (defined by the interior of the stationary limit, $r_s = M + \sqrt{M^2 - a^2\cos^2\theta}$, note that there are 40 grid points between $r = 1.203M$ and r_s at $\theta = \pi/2$). This radial energy beam diminishes precipitously just outside the horizon, near the equatorial plane in all three time steps. The region in which S^r diminishes is adjacent to a region of strong S^θ that originates in the inertially dominated accretion flow in the inner ergosphere, $1.2M < r < 1.6M$ (this region is resolved by 28 radial grid zones). In fact, if one looks at the conservation of energy equation, the term $\partial(S^\theta)/\partial\theta$ is sufficiently large to be the source of $\partial(S^r)/\partial r$ at the base of the radial beam in all three frames. This does not preclude the transfer of energy to and from the plasma. It merely states that the magnitude is sufficient to source S^r. In general, the hydrodynamic energy flux is negligible in the funnel. In order to illustrate this, contours of S^θ are superimposed on the color plots of S^r. The contour levels are chosen to be 2/3 and 1/3 of the maximum value of S^θ emerging from the dense equatorial accretion flow. One clearly sees S^θ switching off where S^r switches on. We conclude that a vertical Poynting flux created in the equatorial accretion flow is the source of the strong beams of S^r. This establishes condition 1 of the Introduction.

The left column of figure 2 contains plots of the magnetic field component, $B^\theta \equiv F_{r\phi}$, at the three time steps. At every location in which S^θ is strong in figure 1, there is a pronounced enhancement in B^θ in figure 2. Recall that the sign of S^θ is not determined by the sign of B^θ. These intense flux patches penetrate the inertially dominated equatorial accretion flow in all three frames. The density contours indicate that the regions of enhanced vertical field greatly disrupt the equatorial inflow. As noted in the introduction, a GHM interaction is likely to occur when the magnetic field impedes the inflow in the ergosphere. The regions of large B^θ are compact compared to the global field configuration of the jet, only $\sim 1.0M - 2.0M$ long. Considering the turbulent, differentially rotating plasma in which they are embedded, these are most likely highly enhanced regions of twisted magnetic loops created by the MRI. The strength of B^θ at the base of the flares is comparable to, or exceeds the radial magnetic field strength. The situation is clearly very unsteady and vertical flux is constantly shifting from hemisphere to hemisphere. The time slice t = 10000 M, although primarily a southern hemisphere event, also has a significant contribution in the northern hemisphere (see the blue fan-like plume of vertical Poynting flux in figure 1). The GHM interaction is provided by the vertical flux that links the equatorial plasma to the relatively slowly rotating plasma of the magnetosphere within the accretion vortex. The vertical flux transmits huge torsional stresses from the accretion flow to the magnetosphere.

Further corroboration of this interpretation can be found by looking at the values of Ω_F in the vicinity of the S^r flares. In a non-axisymmetric, non-time stationary flow, there is still a well defined notion of Ω_F: the rate at which a frame of reference at fixed r and θ would have to rotate so that the poloidal component of the electric field, $E^\perp$, that is orthogonal to the poloidal magnetic field, B^P, vanishes. This was first derived in Punsly (1991) (see the extended discussion in Punsly (2001) for the various physical interpretations), and has recently been written out in B-L coordinates in Hawley and Krolik (2006) in terms of the plasma three-velocity, v^i and the Faraday tensor as

$$\Omega_F = v^\phi - F_{\theta r}\frac{g_{rr}v^r F_{\phi\theta} + g_{\theta\theta}v^\theta F_{r\phi}}{(F_{\phi\theta})^2 g_{rr} + (F_{r\phi})^2 g_{\theta\theta}} \ . \tag{2-1}$$

This expression was studied in the context of the simulation KDH, $a/M = 0.95$, in Hawley and Krolik (2006). They found that a long term time and azimuth average yielded $\Omega_F \approx 1/3\Omega_H$ and there was no enhancement at high latitudes as was anticipated by Phinney (1983). The t = 10000 M time slice of KDH was generously provided to this author. At t = 10000 M, there are no strong flares emerging from the equatorial accretion flow. Inside the funnel at $r < 10M$, at t=10000 M, $0 < \Omega_F < 0.5\Omega_H$.

The right hand column of figure 2 is Ω_F plotted at three different time steps for KDJ. By comparison to figure 1, notice that each flare in S^r is enveloped by a region of enhanced

Ω_F, typically $0.7\Omega_H < \Omega_F < 1.2\Omega_H$. The regions of the funnel outside the ergosphere are devoid of large flares in S^r and typically have $0 < \Omega_F < 0.5\Omega_H$, similar to what is seen in KDH.. Unlike KDH, there are huge enhancements in Ω_F at lower latitudes in the funnel. It seems reasonable to associate this large difference in the peak values of Ω_F in KDJ and KDH (at t= 10000 M) with the spatially and temporally coincident flares in S^r that occur in KDJ. Furthermore, this greatly enhanced value of Ω_F indicates a different physical origin for Ω_F in the flares than for the remainder of the funnel or in KDH at t = 10000 M. The most straightforward interpretation is that it is a direct consequence of the fact that the flares originate on magnetic flux that is locked into approximate corotation with the dense accreting equatorial plasma (i.e., the inertially dominated equatorial plasma anchors the magnetic flux). In the inner ergosphere, frame dragging enforces $0.7\Omega_H < d\phi/dt < 1.0\Omega_H$ on the accretion flow. This establishes condition 2 of the Introduction.

3. Discussion

In this Letter we showed that in the last three data dumps of the 3-D MHD numerical simulation, KDJ, the dominant source of Poynting flux originated near the equatorial plane deep in the ergopshere. The phenomenon is unsteady and is triggered by large scale vertical flux that is anchored in the inertially dominated equatorial accretion flow. The situation typifies the ergospheric disk in virtually every aspect, even though there is an intense accretion flow. There is one exception, unlike the ergospheric disk, the anchoring plasma rarely achieves the global negative energy condition that is defined by the four-velocity, $-U_t < 0$, because of the flood of incoming positive energy plasma from the accretion flow. The plasma attains $-U_t < 0$ only near the base of the strongest flares seen in the $\phi =$ constant slices.

The switch-on of a powerful beam of S^r outside the horizon at $r \approx 1.3M$ in the $a/M = 0.995$ simulation, KDE, of Krolik et al (2005) was demonstrated in Punsly (2006a). It seems likely the the source of S^r in KDE is S^θ from an ergopsheric disk. The ergospheric disk appears to switch on at $a/M > 0.95$ as evidenced by the factor of 3 weaker Poynting flux in KDH. Furthermore, if the funnel opening angle at the horizon in KDH at t= 10000 M is typical within $\pm 5^\circ$ then figure 5 and table 4 of Hawley and Krolik (2006) indicate that only 35% to 40% of the funnel Poynting flux at large distances is created outside the horizon during the course of the simulation. A plausible reason is given by the plots of B^θ in figure 2. The vertical magnetic flux at the equatorial plane is located at $r < 1.55M$. The power in the ergospheric disk jet $\sim [B^\theta(SA)(\Omega_H)]^2$, where SA is the proper surface area of the equatorial plane threaded by vertical magnetic flux (Semenov et al 2004; Punsly 2001). The proper surface area in the ergospheric equatorial plane increases dramatically

at high spin, diverging at $a = M$. For example, between the inner calculational boundary and 1.55 M the surface area is only significant for $a/M > 0.95$ and grows quickly with a/M, exceeding twice the surface area of the horizon for $a/M = 0.99$. Thus, if B^θ in the inner ergosphere were independent of spin to first order, then a strong ergospheric disk jet would switch-on in the 3-D simulations at $a/M > 0.95$. Note that if the inner boundary were truly the event horizon instead of the inner calculational boundary then this argument would indicate that the ergospheric disk would likely be very powerful even at $a/M = 0.95$ and the switch-on would occur at $a/M \approx 0.9$. The implication is that a significant amount of large scale magnetic flux threading the equatorial plane of the ergopshere (which implies a large black hole spin based on geometrical considerations) catalyzes the formation of the most powerful Poynting jets around black holes. Thus, we are now considering initial conditions in simulations that are conducive to producing significant vertical flux in the equatorial plane of the ergosphere.

It should be noted that 2-D simulations from a similar initial state of torii threaded by magnetic loops have been studied in McKinney and Gammie (2004). However, the magnetic flux evolution can be much different in this setting as discussed in Punsly (2006a) and poloidal flux configurations conducive to GHM could be highly suppressed. In summary, there are no interchange instabilities, so flux tubes cannot pass by each other or move around each other in the extra degree of freedom provided by the azimuth. Thus, there is a tendency for flux tubes to get pushed into the hole by the accretion flow. This is in contrast to the formation of the ergospheric disk in Punsly and Coroniti (1990) in which buoyant flux tubes are created by reconnection at the inner edge of the ergospheric disk and recycle back out into the outer ergosphere by interchange instabilities. Ideally, a full 3-D simulation with a detailed treatment of resistive MHD reconnection is preferred for studying the relevant GHM physics.

I would like to thank Jean-Pierre DeVilliers for sharing his deep understanding of the numerical code and these simulations. I was also very fortunate that Julian Krolik and John Hawley were willing to share their data in the best spirit of science.

REFERENCES

Blandford, R. and Znajek, R. 1977, MNRAS. **179**, 433

De Villiers, J-P., Hawley, J., Krolik, 2003, ApJ **599** 1238

De Villiers, J-P., Hawley, J., Krolik, J.,Hirose, S. 2005, ApJ **620** 878

De Villiers, J-P., Staff, J., Ouyed, R.. 2005, astro-ph 0502225

Hawley, J., Krolik, K. 2006, ApJ **641** 103

Hirose, S., Krolik, K., De Villiers, J., Hawley, J. 2004, ApJ **606**, 1083

Krolik, K., Hawley, J., Hirose, S. 2005, ApJ **622**, 1008

McKinney, J. and Gammie, C. 2004, ApJ **611** 977

McClintock, J.E. et al 2006, ApJ **652**, 518

Phinney, E.S. 1983, PhD Dissertation University of Cambridge.

Punsly, B., Coroniti, F.V. 1990, ApJ **354** 583

Punsly, B. 1991, ApJ **372** 424

Punsly, B. 2001, *Black Hole Gravitohydromagnetics* (Springer-Verlag, New York)

Punsly, B. 2006, MNRAS **366** 29

Punsly, B. 2006, ApJL **651** L17

Punsly, B. 2007, MNRAS **374** 10

Semenov, V., Dyadechkin, S. and Punsly, B. 2004, Science **305**978

Thorne, K., Price, R. and Macdonald, D. 1986, *Black Holes: The Membrane Paradigm* (Yale University Press, New Haven)